32nd EPS Conference on Plasma Phys. Tarragona, 27 June - 1 July 2005 ECA Vol.**29C**, P-1.052 (2005)

Electron heat transport dependence on plasma shape and collisionality in EC heated L-mode TCV plasmas

Y. Camenen, A. Pochelon, A. Bottino, I. Pavlov, R. Behn, S. Coda, T.P. Goodman, M.A. Henderson, J.-M. Moret, L. Porte, O. Sauter, G. Zhuang

Centre de Recherches en Physique des Plasmas CRPP,

Ecole Polytechnique Fédérale de Lausanne EPFL,

Association EURATOM-Confédération Suisse, 1015 Lausanne, Switzerland

The study of electron heat transport dependence on controllable plasma parameters is strongly motivated by the needs to predict the plasma energy confinement in future magnetic confinement devices and improve it towards the conditions required for plasma ignition. This paper investigates the role of plasma shape - focusing on plasma triangularity - and plasma collisionality on the local electron heat transport properties of L-mode plasmas. Global confinement studies in Ohmic [1, 2] and in centrally EC heated L-mode plasmas [3, 4] showed indeed the beneficial role of low or negative triangularity on the electron energy confinement time. Moreover, plasma collisionality has been shown recently to play an essential role in particle transport through the stabilization of the trapped electron mode (TEM) at high collisionality [5, 6] and is expected to also influence electron heat transport.

The present experiments are performed in moderately elongated L-mode plasmas, $\kappa = 1.6$, in limiter configuration. The plasma triangularity is varied from negative to positive values, $-0.4 < \delta < 0.4$, using the unique shaping capabilities of the TCV tokamak ($R_0 = 0.88\,\mathrm{m}$, $a = 0.25\,\mathrm{m}$). We define the normalized radius as the square root of the normalized plasma volume: $\rho = \sqrt{V/V_{\mathrm{LCFS}}}$. Both the electron temperature T_e and the normalized electron temperature gradient R/L_{T_e} are varied over an unusually large range by depositing up to 1.8 MW of radially localized X2 EC heating power at two different radial locations: one off-axis at $\rho_1 = 0.35$, just outside the $q = 1$ surface, and one far off-axis, at $\rho_2 = 0.7$ [7]. The density range is fixed to $0.8 < \bar{n}_\mathrm{e} < 1.8 \cdot 10^{19}\,\mathrm{m}^{-3}$, such as to avoid excessive refraction of the EC beams while also ensuring full single pass absorption for the far off-axis deposition.

Cross field electron heat transport is studied by calculating the electron thermal diffusivity χ_e defined by $Q_\mathrm{e} = -n_\mathrm{e}\chi_\mathrm{e} < |\nabla\rho|^2 > \frac{\partial T_\mathrm{e}}{\partial \rho}$, where Q_e is the electron heat flux and where the brackets indicate an average over the flux surface. The electron density n_e and electron temperature T_e profiles are measured by Thomson scattering every 25 ms and averaged over 300 ms after stationary internal inductance l_i is reached. The EC power, dominating the power balance, is obtained from the TORAY-GA linear ray tracing code, the ion temperature profile from the

Charge Exchange Recombination Spectroscopy diagnostic and the radiated power from XUV-bolometer photodiodes. The plasma current density profile is calculated using the transport code PRETOR in interpretative mode, consistently taking into account the experimental pressure profiles and the current density sources, Ohmic and bootstrap (EC driven current negligible), to reconstruct the magnetic equilibrium. The Z_{eff} value is estimated so as to match the value of the calculated total plasma current with the value of the experimental one. More details concerning the diagnostics and methods used for the analysis are given in [8].

In TCV, the electron heat transport strongly decreases with increasing collisionality for the entire range of plasma triangularities explored, as shown in Fig. 1a and 1b, where the electron heat diffusivity calculated at mid-radius is plotted as a function of the effective collisionality $\nu_{\mathrm{eff}} = \frac{\nu_{\mathrm{ei}}}{\omega_{\mathrm{De}}} \approx 0.1R\frac{n_{\mathrm{e}}Z_{\mathrm{eff}}}{T_{\mathrm{e}}^2}$. Concerning the effect of plasma shape, χ_{e} does not depend significantly on triangularity for positive δ values, but clearly decreases with decreasing triangularity for negative δ values. As the gyro-Bohm scaling predicts an electron heat diffusivity χ_{e} proportional to $f_{gB} = \frac{T_{\mathrm{e}}^{3/2}}{aB^2}$, we plot the gyro-Bohm normalized heat diffusivity χ_{e}/f_{gB} as a function of ν_{eff} in Fig. 1c and 1d to check whether the variation of χ_{e} with ν_{eff} is only due to a gyro-Bohm dependence on the electron temperature. A decrease of χ_{e}/f_{gB} is observed with increasing ν_{eff}. The χ_{e} dependence on $T_{\mathrm{e}}^{3/2}$ of the gyro-Bohm scaling could be correct, but has therefore to be completed with a ν_{eff} dependence. The reduction of electron heat transport with decreasing δ is still visible, and even more pronounced, with the gyro-Bohm normalization. In the set of experiments of Fig. 1a and 1c, the plasma triangularity was varied at constant plasma current, $I_{\mathrm{p}} = 220\,\mathrm{kA}$, leading to a small variation of the edge safety factor from $q_{95} = 4.7$ at $\delta = 0.2$ to $q_{95} = 5.4$ at $\delta = 0.4$. The EC power distribution was changed from far off-axis to off-axis deposition to cover a large range of $R/L_{T_{\mathrm{e}}}$ values, from 4 to 20, at mid-radius. No dependence of χ_{e} on $R/L_{T_{\mathrm{e}}}$ is observed at high $R/L_{T_{\mathrm{e}}}$ values, which is described in [7, 8] and

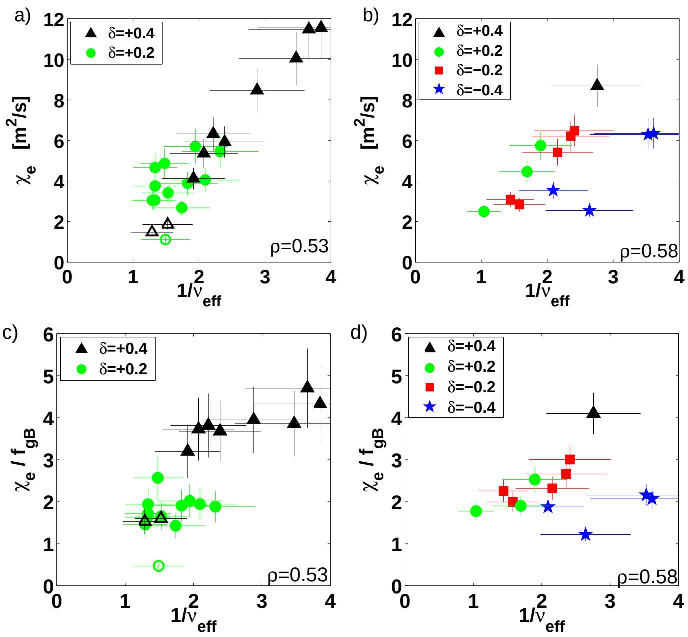

Figure 1: *Electron heat transport reduction at high plasma collisionality and negative plasma triangularity.*

suggested by the small scattering of the data in Fig. 1a and 1c. In the set of experiments of Fig. 1b and 1d, the plasma triangularity was varied over a large range keeping the edge safety factor constant, $q_{95} = 3.5$, by changing parabolically I_p with δ with a minimum around $\delta = -0.2$. The EC power deposition was kept constant at ρ_1, leading to high R/L_{T_e} values.

Local gyro-fluid GLF23 and global collisionless gyro-kinetic LORB5 linear simulations both indicate that for most experimental conditions of Fig. 1, the dominant instability is a TEM mode (full symbols), except at the lowest R/L_{T_e} values, obtained with far off-axis ECH, where it is an ITG mode (open symbols) [8]. The experimental decrease of χ_e with plasma collisionality is consistent with the expected stabilization of TEM modes at high collisionality shown in GLF23 simulations. Moreover the experimental finding that χ_e/f_{gB} does not depends on R/L_{T_e} for $R/L_{T_e} > 10$ supports the recent quasi-linear simulations of TEM modes [9].

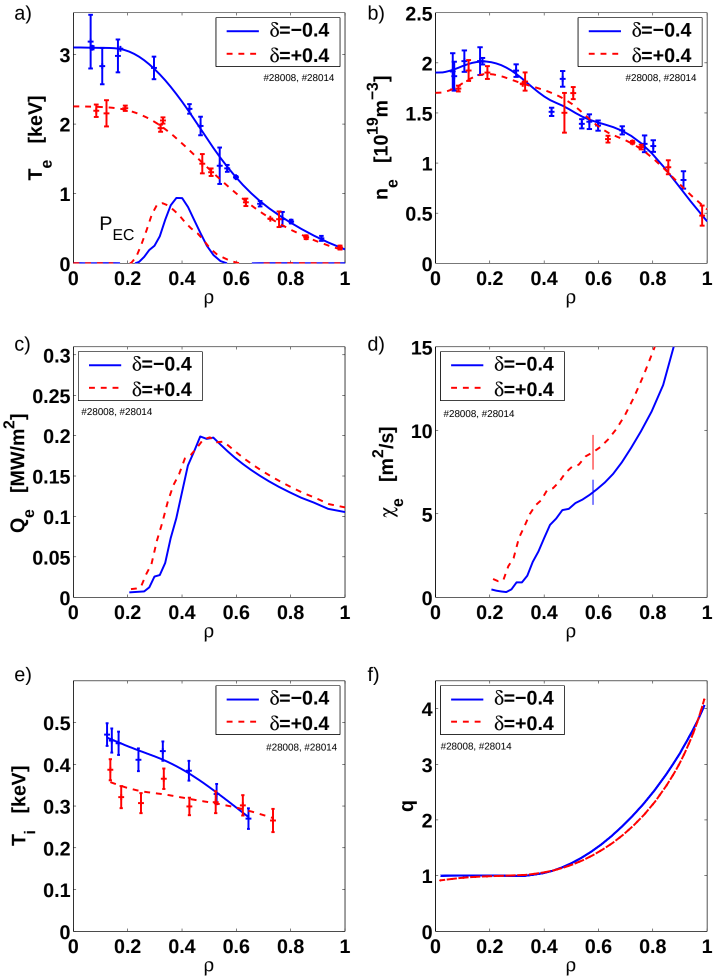

Figure 2: *Detailed comparison of negative and positive triangularity plasmas showing the electron heat transport reduction towards negative triangularities.*

To investigate the effect of plasma triangularity δ on electron heat transport, we also extensively compare two plasmas with negative and positive triangularities, $\delta = -0.4$ and $\delta = +0.4$, keeping constant other controlled plasma parameters, Fig. 2. The line averaged density, $\bar{n}_e = 1.4 \cdot 10^{19}\,\mathrm{m}^{-3}$, as the total deposited EC power, $P_{EC} = 1.3\,\mathrm{MW}$, and the edge safety factor, $q_{95} = 3.5$, are maintained constant. A clear reduction of electron heat transport is observed towards negative triangularities: the electron temperature is substantially higher and the electron heat diffusivity lower at $\delta = -0.4$

than at $\delta = +0.4$. The ion temperature follows the same trend than the electron temperature. In the two cases, the electron density and safety factor profiles are similar. The electron heat flux profiles are also similar, except for $\rho < 0.45$ due to a slightly more off-axis EC power deposition at $\delta = -0.4$ as compared to $\delta = +0.4$. To get information from heat pulse propagation, we performed square wave EC power modulation ($f = 523\,\text{Hz}$, $\frac{\Delta P_{\text{EC}}}{P_{\text{EC}}} = 40\%$, $P_{\text{EC}} = 1.3\,\text{MW}$). The amplitude and phase profiles of the Fourier transform of the electron temperature measured by the ECE diagnostic are shown in Fig. 3. The corresponding heat pulse heat diffusivity, computed at $\rho = 0.58$ in slab geometry, is $9\,\text{m}^2/\text{s}$ at $\delta = -0.4$ and $7\,\text{m}^2/\text{s}$ at $\delta = +0.4$. The local electron heat transport reduction towards negative δ also improves the global energy confinement. Reducing the triangularity from $\delta = +0.4$ to $\delta = -0.4$, the electron energy confinement time τ_{Ee} increases from 3.6 to 5.3 ms and the electron energy confinement time normalized to the RLW model prediction increases from 1.5 to 2.2. As a consequence only half of the EC power used at a triangularity of $\delta = +0.4$ ($P_{EC} = 1.3\,\text{MW}$) has been required at $\delta = -0.4$ ($P_{EC} = 0.6\,\text{MW}$) to obtain the same temperature profile, keeping constant the line averaged density and edge safety factor. The reduction of electron heat transport towards smaller plasma triangularity is significant and has a strong impact on the global plasma confinement.

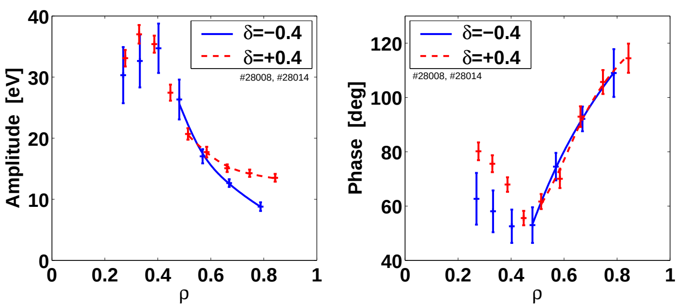

Figure 3: *Amplitude and phase profiles of the Fourier transform of the electron temperature measured by ECE.*

References

[1] J.-M. Moret, S. Franke, H. Weisen et al., Phys. Rev. Lett. **79**, 2057 (1997)

[2] H. Weisen, J.-M. Moret, S. Franke et al., Nucl. Fusion **37**, 1741 (1997)

[3] A. Pochelon, T.P. Goodman, M.A. Henderson et al., Nucl. Fusion **39**, 1807 (1999)

[4] A. Pochelon et al., Proc. 26th EPS Conf. (Maastricht, Netherlands) **23J**, 1089 (1999)

[5] C. Angioni et al., Phys. Rev. Lett. **90** 205003 (2003)

[6] H. Weisen, A. Zabolotsky et al., Nucl. Fusion **45** (2005)

[7] A. Pochelon, Y. Camenen et al., Proc. 20th IAEA Fusion Energy Conference (Vilamoura, Portugal), IAEA-CN-116/EX/9-1 (2004)

[8] Y. Camenen, A. Pochelon et al., submited to Plasma Phys. Control. Fusion (2005)

[9] A.G. Peeters et al., Phys Plasmas **12** 022505 (2005)